

DAA/LANGLEY

P.19

Department of Aerospace Engineering
The Pennsylvania State University
University Park, PA 16802

IN-02

69626-CR

PJ 304212

Annual Progress Report on
NASA Grant No. NAG-1-657

(NASA-CR-180558) REYNOLDS STRESS CLOSURE IN
JET FLOWS USING WAVE MODELS Annual Progress
Report (Pennsylvania State Univ.) 19 p
Avail: NTIS HC A02/MF A01 CSCL 01A

N87-26861

Unclas

G3/02 0069626

Reynolds Stress Closure in Jet Flows
Using Wave Models

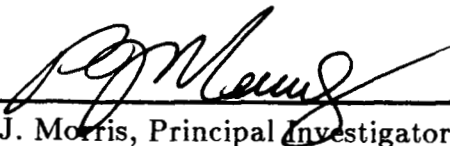
sponsored by

National Aeronautics and Space Administration

Langley Research Center
Hampton, VA 23665

Submitted by:

Date:



5/4/87

P. J. Morris, Principal Investigator
Professor of Aerospace Engineering
233-L Hammond Building
University Park, PA 16802
(814) 863-0157

Introduction

During the first year of the research program efforts have concentrated on the development of the numerical methods that will form the computational part of the turbulence closure scheme. A wave model has been developed for the two-dimensional shear layer. This configuration is being used as a test case for the closure schemes. Various numerical schemes have been examined to give efficient solutions of the Rayleigh equation for this geometry. These include both spectral and finite difference methods. Secondly, numerical methods are under development to solve the non-separable Rayleigh equation. This solution is required for the closure scheme in more complex geometries. A model problem has been used to assist in the algorithm development. Two-dimensional spectral methods and a hybrid spectral/finite difference technique have been developed. An analytic solution of the Rayleigh equation for a basic elliptic flow has been obtained. This will be used to verify the stability codes developed for arbitrary geometries. Other numerical methods for solving the Rayleigh equation based on the boundary element technique have also been examined. These solutions are forming the basis of a model for the shock structure in jets of arbitrary geometry. These activities are described briefly below.

Turbulence Closure in a Mixing Layer

A turbulence closure scheme using a wave model is being developed. An incompressible two-dimensional free mixing layer has been chosen as a test case. In the future the model will be used to predict the mean velocity and temperature fields in jets and describe the characteristic frequency and wavelength properties of the fluctuating flow field.

Since the large-scale coherent structures develop spatially, they may be best represented by spatial instability waves characterized by the solution of the Rayleigh equation. At present the Reynolds stress associated with the dominant large-scale structure is mod-

eled by the spatially-developing most unstable mode. Future extensions of this model involve the inclusion of a wider frequency spectrum.

Both the traditional shooting technique and the methods proposed by Bridges and Morris (1984) have been used in the solution of the Rayleigh equation. It has been found that a Chebyshev polynomial of relatively high order is needed to obtain accurate solutions if the tau method is used. The matrix operations involved in this technique, which is the discretization method used by Bridges and Morris, consume a relatively large amount of computer time. This is particularly undesirable as this solution is only one part of the closure scheme. Different ways to construct the coefficient matrices have been investigated. These include:

- (1) a finite difference method and
- (2) a Chebyshev collocation method.

Eigenvalues of higher accuracy than those obtained using the tau method have been obtained with the order of the matrices less than half of those in the tau method. The results for a mixing layer with a hyperbolic tangent mean velocity profile are shown in Table 1. The eigenfunctions are relatively insensitive to the precision with which the eigenvalues are obtained so that it is unnecessary to obtain highly accurate eigenvalues. It would also decrease the efficiency of the turbulence closure scheme.

The wave model has been applied locally to a mixing layer with the mean velocity profile obtained from an analytic curve fit to measured data by Patel (1973). The calculated Reynold stresses are shown in Fig. 1. Note that the maximum value assigned to the instability wave stresses is based on the measured data and neglects the contributions from the small-scale turbulence. The distribution shows that there are regions of negative turbulent production associated with the large-scale structures. This was observed by Komori and Ueda(1985). Moreover, it is clear from Fig. 1 that the contributions to the Reynolds stress from the small-scale turbulent motion must be accounted for in the model.

REYNOLD STRESS FOR FREE SHEAR LAYER (PAT./W. 14)

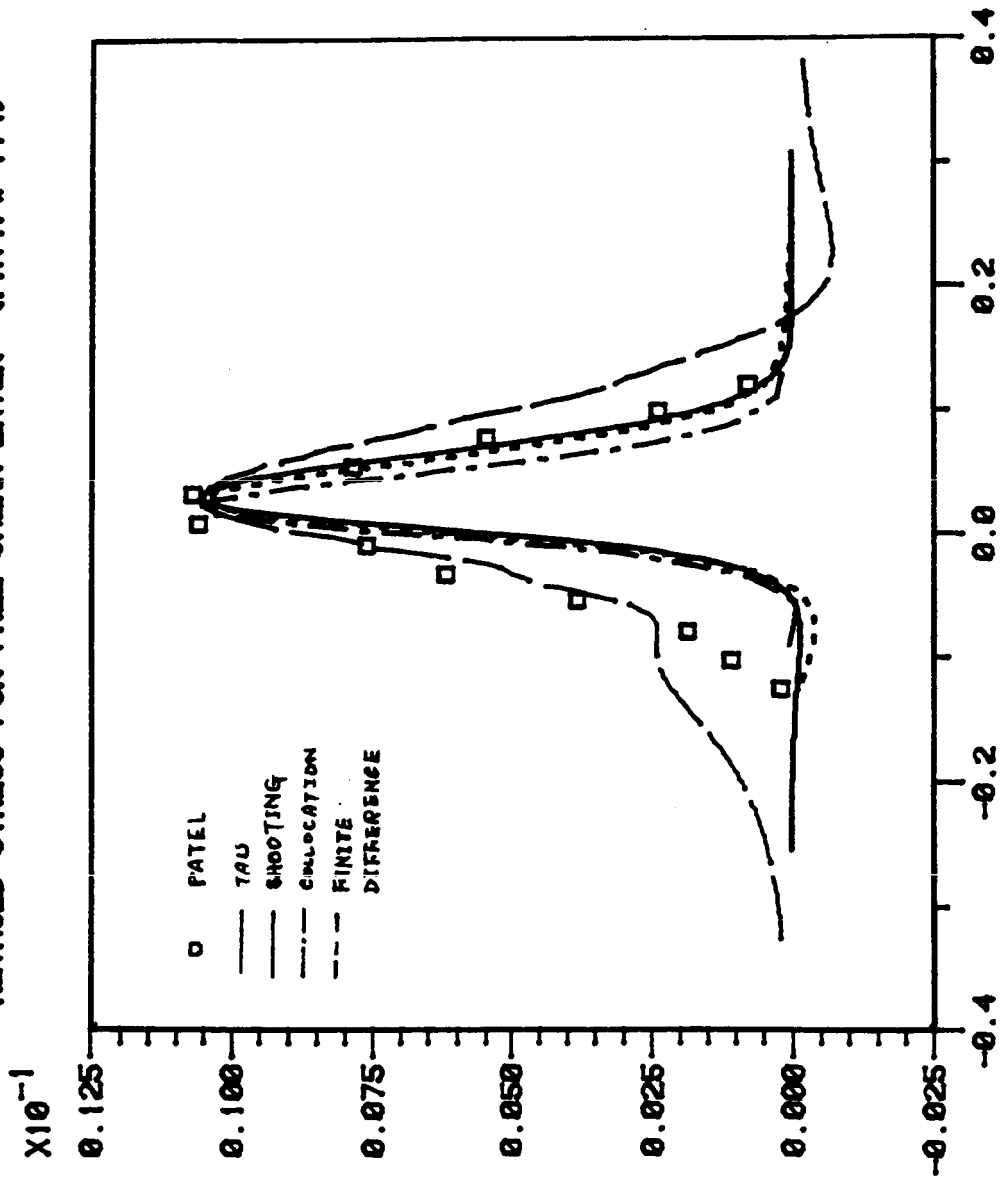


Figure 1. Calculation of Reynolds Stress Using Different Numerical Schemes

The inclusion of the interaction between the the large-scale and the small-scale turbulence and the contributions of the latter to the flow development is clearly a requirement for any viable turbulence model.

Method	N	Frequency	Eigenvalue
Tau	26	0.2	(0.367, -0.219)
Finite Difference	11	0.2	(0.383, -0.221)
Collocation	11	0.2	(0.389, -0.221)
Michalke(1966)		0.2	(0.382, -0.227)

Table 1. Calculation of Eigenvalues

It is recognized that turbulence comprises fluctuating motions with a wide spectrum of length and time scales and that different turbulent interactions are associated with different parts of the spectrum. Following the general ideas proposed by Hanjalic et al (1980) we assume that the turbulent kinetic energy spectrum may be divided into parts associated with the large-scale structures and that associated with the residual motions. Since the large-scale structures, based on the present wave model, dominate the dynamics mechanism of a free shear flow, we further assume that the large-scale structures are most effective in extracting energy from the mean flow. The turbulent energy is then transported to the other scales of motion through vortex stretching or higher-order instabilities and is then dissipated by viscous effects. A spectrum division similar to Hanjalic et al may be proposed as sketched in Fig. 2. k_l , k_s denote the turbulent kinetic energies associated with the large- and small-scale range and ϵ_l denotes the kinetic energy transfer rate across the inertial subrange. ϵ represents the rate of energy dissipation in the small-scale structures. The transport equations for the kinetic energies may be written as

$$\frac{Dk_l}{Dt} = -\overline{\tilde{u}_i \tilde{u}_j} \frac{\partial U_i}{\partial x_j} - \epsilon_l, \quad (1)$$

$$\frac{Dk_s}{Dt} = \epsilon_l - \epsilon. \quad (2)$$

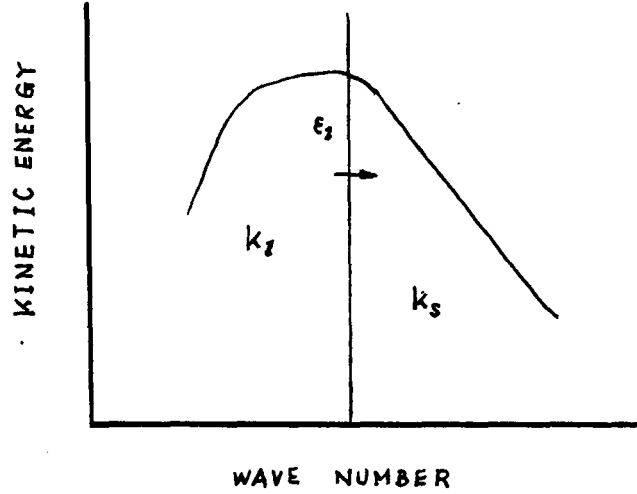


Figure 2. Sketch of turbulent energy spectrum

An eddy viscosity hypothesis may be used to model the contribution to the Reynolds stress by the small-scale motions.

$$-\overline{u'_i u'_j} = C_1 u l_s \tilde{S}_{ij},$$

where u and l_s are the velocity and length scales associated with the small-scale motion.

Additional assumptions are made for the small length and velocity scales,

$$u \sim k_s^{1/2},$$

$$l_s \sim u \tau \sim k_s^{3/2} / \epsilon,$$

where τ is the time scale for the small-scale motions. Equation (2) can then be used to solve for k_s , providing that the large-scale characteristics have been obtained from the

wave model and the rate of viscous dissipation is related to the rate of large-scale energy production by $\epsilon \sim k_t^{3/2} / l$. Note that the latter assumption is equivalent to

$$l_s \sim l (k_s/k_t)^{3/2}.$$

Extensions to this rather simple formalism are being examined. These include the extension of the *Algebraic Reynolds Stress Closure* to a multiple-scale decomposition of the turbulence. This extended model and the simpler model described here will next be applied to a calculation of the development of the two-dimensional mixing layer.

2. Solution of the Non-Separable Rayleigh Equation

This phase of research has centered on developing new, and improving existing, numerical methods to solve the non-separable Rayleigh equation.

2.1 Review of Initial Progress - The first step in the solution of the Reynolds-averaged compressible equations of motion for jets of arbitrary geometry using a wave model is the description of the hydrodynamic stability of such flows. This requires the solution of a non-separable form of Rayleigh equation. The most unstable eigensolutions may then be used to model the Reynolds stress associated with the large-scale structures.

A method has been developed to determine the eigensolutions of the Rayleigh equation in flows of arbitrary geometry. The equation to be solved is:

$$(\Delta - \alpha^2)\hat{p} + (2\alpha/\Omega)\nabla W \cdot \nabla\hat{p} = 0 \tag{3}$$

with boundary conditions:

$$\hat{p} \text{ is finite and } \hat{p} \rightarrow 0 \text{ at infinity}$$

where \hat{p} is the pressure fluctuation, $W(x, y)$ is the axial mean velocity, α is the axial wavenumber (the complex eigenvalue), ω is the wave frequency, and $\Omega = \omega - \alpha W$.

In order to test various numerical algorithms for solving this problem a model problem with a known analytic solution has been posed. The boundary value problem is given by:

$$\Delta\phi - 2\alpha\omega(\partial_x\phi + \partial_y\phi) - 2\alpha^2\phi = 0 \quad (4)$$

with,

$$\phi = 0 \quad \text{on} \quad \partial\Omega$$

where

$$\Omega := \{(x, y) \in \mathbf{R}^2 \mid -1 \leq x, y \leq 1\}$$

The method that has been used to determine the eigenvalues α is a *spectral method* using a two-dimensional Chebyshev series approximation of the form:

$$\phi(x, y) = \sum \sum \phi_{mn} T_n(x) T_m(y). \quad (5)$$

Here the summations are taken from 0 to N .

The determination of α goes as follows: i) The P.D.E. is integrated to eliminate all derivatives of the dependent variable. ii) This integral equation is discretized using the Chebyshev series, equation (5). iii) The boundary conditions are discretized. iv) Steps ii) and iii) reduce to the problem of determining all α such that:

$$\det[\mathbf{A}\alpha^2 + \mathbf{B}\alpha + \mathbf{C}] = 0 \quad (6)$$

where \mathbf{A} , \mathbf{B} , and \mathbf{C} are $(N + 1)^2 \times (N + 1)^2$ matrices depending on the discretization. v) Equation (6) is solved using globally or locally convergent schemes.

2.2 Review of Current Research - Logically, the next step is to generalize the Chebyshev integral method from the model problem (4) to the Rayleigh equation (3).

However, this transition is complicated by the non-constant coefficients present in (3). To realize the problem, notice that in general the variable coefficients of the Rayleigh equation must be expanded in infinite series of the form (5). Then the coefficient series must be multiplied by the respective series approximating a term in the Rayleigh equation. Algebraically, the multiplication of multiple infinite series is very complicated and the resulting formulas are tedious to code. Therefore, a spectral method is sought to solve the Rayleigh equation which avoids the algebraic complications of multiplying multiple infinite series together. Such a method is outlined below.

Another difficulty associated with the solution scheme developed for the model problem (4) is the size of the resulting lambda matrix, (6). It is anticipated that a typical value of N will lead to a very large matrix. Hence, from a computational viewpoint it would be advantageous to reduce the order of the lambda matrix. Currently, methods combining finite differences and pseudospectral approximations are being developed. These methods have the potential to reduce the order of the lambda matrix from $(N + 1)^2 \times (N + 1)^2$ to $(N + 1) \times (N + 1)$. Schemes combining finite differences and spectral approximations, i.e., hybrid schemes, will be discussed in section 2.2.2.

2.2.1 Pseudospectral Chebyshev Methods - Let \mathbf{L} denote the partial differential operator associated with the model problem (4). A scheme is sought to determine the complex wave numbers α of the model problem such that

$$\mathbf{L}\phi_N(\mathbf{x}_{ij}, \omega, \alpha) = 0, \tag{7}$$

is satisfied exactly, where ϕ_N is a pseudospectral approximation of the solution. Here, the frequency ω is fixed, and \mathbf{x}_{ij} are collocation points in Ω for $0 \leq i, j \leq N$ defined by:

$$\begin{aligned} \mathbf{x}_{ij} &= (x_i, y_j), \\ &= (\cos[\pi i/N], \cos[\pi j/N]). \end{aligned}$$

Furthermore, ϕ_N is defined by,

$$\phi_N(x, y) = \sum \sum \phi(x_{ij}) f_i(x) f_j(y), \quad (8)$$

where $f_j(z)$ ($z = x$ or y) is given by,

$$f_j(z) = ((1 - z^2) T'_N(z) (-1)^{j+1}) / (c_j N^2 (z - z_j)), \quad (9)$$

with $c_0 = c_N = 2$, and $c_j = 1$ for $j = 1, \dots, N - 1$.

The discretization of eqn. (4) is then given by evaluating eqn. (7) at the collocation points in the interior of Ω and combining these equations with eqn. (8) satisfied at the collocation points on the boundary of Ω . The advantage of the pseudospectral Chebyshev method becomes clear when the operator L is defined to be the Rayleigh operator. Instead of expanding the variable coefficients of L as an infinite series, the coefficients are simply evaluated at the collocation points. Thus, the algebraic problem encountered in the integral method is avoided.

2.2.2 Hybrid Schemes - In order to reduce the order of the discretization matrix, resulting from a multiple series expansion, one variable expansions are currently being used to develop a method to solve the model problem. In general, a one variable series will generate a smaller discretization matrix.

Consider a solution of the form:

$$\phi_N(x, y) = \sum a(x_i, y) f_i(x). \quad (10)$$

Here the summation is taken from 0 to N . Moreover, the f_i 's are functions which may be used to approximate ϕ .

To outline a hybrid scheme, let the functions, f_i , in eqn. (10) be defined by eqn. (9). Therefore, eqn. (10) provides a pseudospectral approximation to the solution in the

x direction. In the y direction, a finite difference scheme will be applied. Let $\nabla^1(y)$ and $\nabla^2(y)$ denote arbitrary finite difference operators in y for the first and second derivatives respectively. Then substituting (10) into the model problem and applying the $\nabla^i(y)$'s gives,

$$[\nabla^2(y) - 2\omega\alpha\nabla^1(y)]\phi_N = [2\omega\alpha\partial_x + 2\alpha^2 - \partial_{xx}]\phi_N, \quad (11)$$

where the operator on the right hand side of eqn. (11) is approximated by the psuedospectral method.

The boundary conditions are established by recasting the boundary value problem in y as an initial value problem. Since the derivative of ϕ with respect to y is unknown along $y = -1$ the solution is constructed as a sum of linear problems for which the initial conditions are

$$\partial_y\phi_N^j(x_i, -1) = \delta_{ij}.$$

The solution on $y = 1$ at the collocation point x_i is given by

$$\phi_N(x_i, 1) = \sum A_j\phi_N^j(x_i, 1). \quad (12)$$

Application of the boundary condition $\phi(x, 1) = 0$ yields a system of homogeneous simultaneous equations for the A_j . For a non-trivial solution the determinant of the coefficient matrix given by these equations must be zero. Only when α is an eigenvalue will this condition be satisfied.

This method is readily extended to the boundary conditions posed for the Rayleigh equation. Casting the non-separable boundary value problem in this way should reduce the operation count by a factor of N^2 and yield a much more efficient evaluation of the eigenvalues.

3. Boundary Element Methods and Shock Structure Tam and his co-workers have shown that both the large-scale coherent structures and the shock structure of jets may be

modeled using a wave analysis. The essential difference between the two cases is that the former are modeled as travelling waves while the latter are standing waves. In this section a numerical method, the boundary element method, has been used to determine the shock structure in jets of arbitrary cross-section modeled by a vortex sheet. In the next stage of the analysis the effect of finite mixing layer thickness and its axial variation will be considered. Modeling this physical problem provides a vehicle to test different numerical methods for the solution of the Rayleigh equation than those described in Section 2 as well as giving additional insight into the physical structure of jets of arbitrary shape.

The shock-structure is to be analyzed for multiple jets of arbitrary shape. The model developed by Tam and his co-workers, e.g. Tam et al (1985), is used here. This model incorporates the effects of a finite thickness mixing layer and the axial flow divergence. We are concerned with solving the equations of linear hydrodynamic stability in which the mean flow characteristics are arbitrary functions in a plane normal to the jet axis or axes and a slowly-varying function of the axial distance. A typical cross-section of a single jet is shown in Fig.3. This defines three regions. In regions I and III the mean flow properties are constant. These regions correspond to the potential core of the jet and the ambient fluid surrounding the jet. Region II represents the jet shear layer in which the mean velocity and density vary.

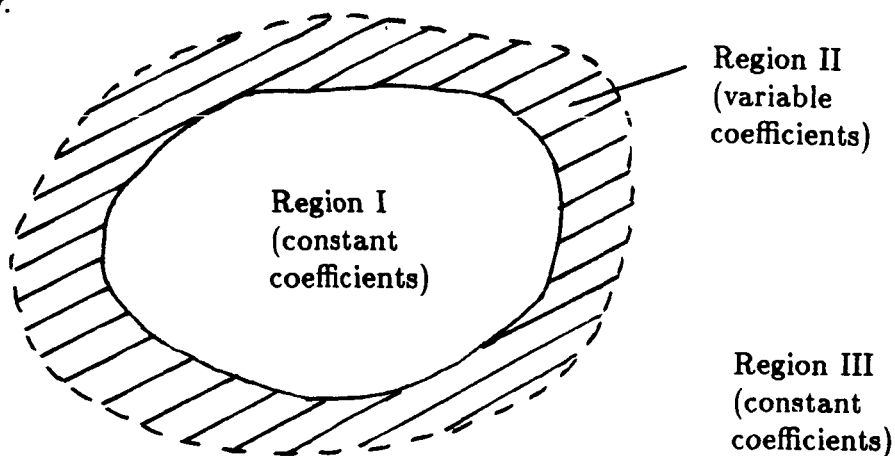


Fig. 3: Sketch of Regions of Jet Cross-Section

The equation for the pressure fluctuations to be solved in these regions is given by,

$$\Delta p + \frac{2k}{(\beta - kU)} \left[\frac{\partial U}{\partial y} \frac{\partial p}{\partial y} + \frac{\partial U}{\partial x} \frac{\partial p}{\partial x} \right] - [k^2 - M^2(\beta - kU)^2] p = 0, \quad (13)$$

where, p is the pressure fluctuation, k is the axial wavenumber, β is the frequency, and $U(x, y)$ is the mean axial velocity. Equation (13) is obtained by taking the divergence of the linearized momentum equation and using the continuity and energy equations.

The analysis of the problem is carried out in the following stages:

- (i) A linear shock cell model is used as a first order approximation to analyze regions I and III. In this model, the mixing layer of the jet, which is assumed to be thin, is approximated by a vortex sheet. This assumption eliminates the need to analyze region II. The details of this model and the solution technique are discussed below.
- (ii) The inclusion of the effects of the finite thickness shear layer and that of axial flow divergence. The inclusion of these effects require a numerical solution in region II. The solution obtained for region II has to be matched with the solutions of regions I and III at the common boundaries.
- (iii) Extension of the model to include the effects of multiple jets of arbitrary cross-sections.

3.1 Vortex Sheet Shock Cell Model - Consider a shock cell system in a jet column bounded by a vortex sheet as shown in Fig. 4. For convenience, a Cartesian coordinate system centered at the nozzle exit with the x -axis in the direction of the jet centerline will be used. The surface of the vortex sheet bounding the fully-expanded jet is given by $S_0(y, z) = 0$. There is no disturbance outside the jet. The linearized equations of motion inside the vortex sheet are:

$$\rho_j \nabla \cdot \mathbf{V} + u_j \frac{\partial \rho}{\partial x} = 0, \quad (14)$$

$$\rho_j u_j \frac{\partial \mathbf{V}}{\partial x} = -\nabla p, \quad (15)$$

$$p = a_j^2 \rho. \quad (16)$$

ρ_j, u_j and a_j are the density, velocity and the speed of sound of the fully expanded jet. ρ, p and \mathbf{V} are the density, pressure and velocity associated with the linear shock cell structure.

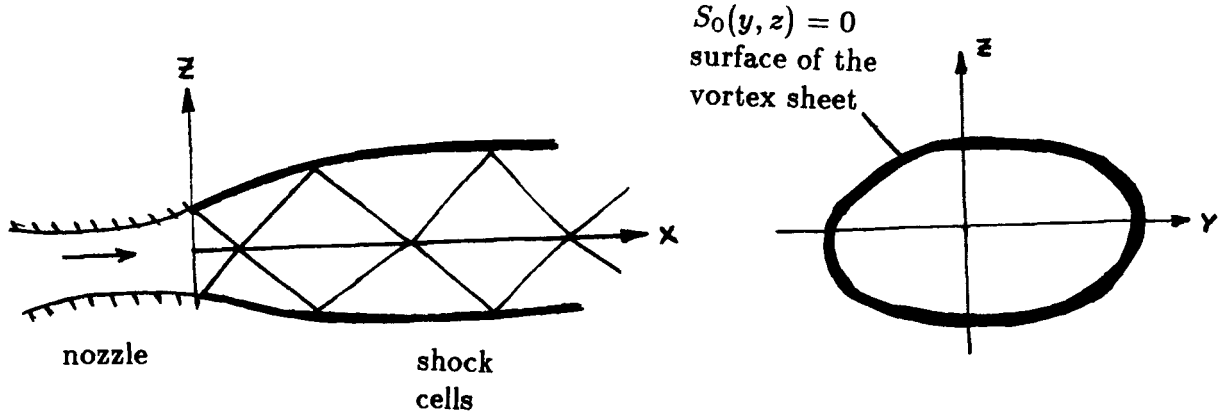


Fig. 4: Vortex Sheet Shock Cell Model

From eqns. (14) to (16) it is found that the pressure p satisfies the equation

$$\nabla^2 p - M_j^2 \frac{\partial^2 p}{\partial x^2} = 0, \quad (17)$$

with $p = 0$ on the boundary $S_0(y, z) = 0$ and at $x = 0$, $p = \Delta p$ inside $S_0(y, z) = 0$ and $\mathbf{V}_\perp = 0$.

A general solution of the vortex sheet shock cell boundary value problem can be found by writing the pressure fluctuation as:

$$p(x, y, z) = \phi(y, z) \cos(kx). \quad (18)$$

where k is an as yet unknown axial wavenumber. The equation for $\phi(y, z)$ may then be written

$$\nabla^2 \phi + \lambda^2 \phi = 0 \quad \text{where,} \quad \lambda^2 = (M_j^2 - 1)k^2, \quad (19)$$

with $\phi = 0$ on $S_0(y, z) = 0$. This is an eigenvalue problem with k as the eigenvalue, which is to be determined.

The **Boundary Element Method** is used to solve the Helmholtz equation (19). This integral technique is particularly suited to problems posed in an arbitrary geometry. The development of the method is discussed below.

Consider an arbitrary domain as shown in Fig. 5 where the boundary is divided into N panels. $\xi = \xi(a_1, a_2)$ are the locations of the node points and $\alpha = \alpha(b_1, b_2)$ are the locations of the mid points of each panel.

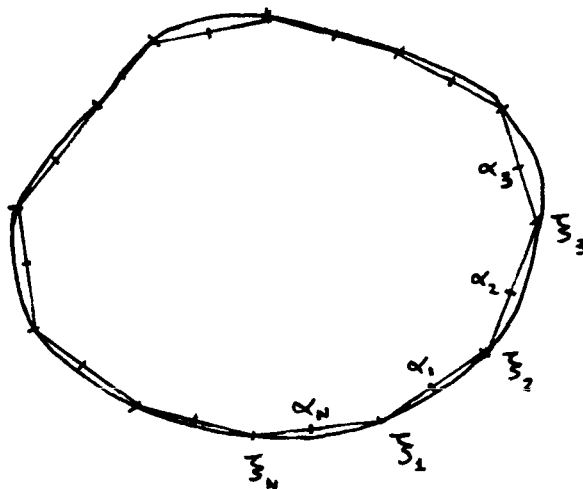


Fig. 5: Sketch of Boundary Divided into Elements

Let $F(x | y)$ be the fundamental solution of the Helmholtz equation, i.e.

$$(\Delta + \lambda^2)F(x | y) = -\delta(x - y), \quad (20)$$

where, $x = (x_1, x_2)$ and $y = (y_1, y_2)$ and x and y are arbitrary. Then,

$$F(x | y) = \frac{i}{4} H_0^{(1)}(\lambda|x - y|)$$

Application of the divergence theorem and noting that ϕ satisfies eqn. (16) and is zero on the boundary yields,

$$\frac{1}{2}\phi(\alpha_i) = \int_{S_0=0} \frac{\partial\phi(\xi)}{\partial\nu} F(\alpha | \xi) d\sigma \quad \text{for } i = 1, 2, 3, \dots, N$$

Approximating $\partial\phi/\partial\nu$ by a constant, say g_i on each arc Γ_i , we obtain,

$$\frac{1}{2}\phi(\alpha_i) = \sum_{j=1}^N g_j \int_{\Gamma_j} F(\alpha_i | \xi) d\sigma,$$

or,

$$\frac{1}{2}\phi(\alpha_i) = \sum_{j=1}^N \mu_{ij}(\lambda) g_j,$$

where,

$$\mu_{ij}(\lambda) = \int_{\Gamma_j} F(\alpha_i | \xi) d\sigma.$$

The approximate eigenvalues λ are obtained from,

$$\det[\mu_{ij}]_{N \times N} = 0$$

Let L_i be the length of the panel on the arc Γ_i . Then,

for $i = j$,

$$\mu_{ij} = \frac{1}{4} \left\{ L_i H_0^{(1)} \left(\frac{\lambda L_i}{2} \right) + \frac{\pi L_i}{2} \left[\mathbf{H}_0 \left(\frac{\lambda L_i}{2} \right) H_1^{(1)} \left(\frac{\lambda L_i}{2} \right) - \mathbf{H}_1 \left(\frac{\lambda L_i}{2} \right) H_0^{(1)} \left(\frac{\lambda L_i}{2} \right) \right] \right\}$$

For $i \neq j$,

$$\mu_{ij}(\lambda) = \frac{i}{4} \left\{ \frac{L_j}{6} \left[H_0^{(1)}(\lambda|\alpha_i - \xi_j|) + 4H_0^{(1)}(\lambda|\alpha_i - \alpha_j|) + H_0^{(1)}(\lambda|\alpha_i - \xi_{j+1}|) \right] \right\},$$

where, $\mathbf{H}(z)$ are Struve functions that can be expressed as a series of Bessel functions.

The eigenvalues are obtained by a local iterative scheme which is given by,

$$\lambda_{k+1} = \lambda_k - 1/f(\lambda_k),$$

where,

$$f(\lambda_k) = \text{Tr}[\mu^{-1}(\lambda_k)\mu'(\lambda_k)],$$

Tr denotes the trace of a matrix and a prime denotes the derivative of the matrix with respect to λ_k .

Thus the eigenvalues can be determined starting from an initial guess.

The Boundary Element Method has been used to solve the vortex sheet shock cell model for rectangular and circular jets. These two geometries are chosen for the reason that their analytical solutions for the eigenvalues are easily obtainable. The numerical and the analytical values are compared for the smallest eigenvalue as this primarily determines the shock cell spacing. The results are shown in Tables II and III.

As is to be expected the number of panels has a great effect on the accuracy and the number of iterations required. A compromise between the accuracy required and the total CPU time has to be reached.

Analytical value of $\lambda = 4.442883$.

Number of Panels	Number of Iterations	$\lambda_{numerical}$	$\lambda_{initial}$	% error
4	29	(5.14421,0.1056)	(4.0,0.0)	15.78
8	11	(4.31998,-0.05169)	(4.0,0.0)	2.77
12	11	(4.40674,-0.02355)	(5.0,0.0)	0.81
20	11	(4.43237,-0.00627)	(5.0,0.0)	0.24
28	12	(4.43795,-0.00243)	(5.0,0.0)	0.11
40	13	(4.44057,-0.00086)	(5.0,0.0)	0.05

Table II: Calculations for a Rectangular Jet

Analytical value of $\lambda = 2.40482$.

Number of Panels	Number of Iterations	$\lambda_{numerical}$	$\lambda_{initial}$	% error
4	28	(3.63751,0.07463)	(3.0,0.0)	51.25
8	12	(2.58661,-0.02283)	(3.0,0.0)	7.60
12	12	(2.47651,-0.00827)	(3.25,0.0)	3.00
20	11	(2.42874,-0.00201)	(2.75,0.0)	1.00
30	12	(2.41510,-0.00062)	(2.75,0.0)	0.40
40	14	(2.41000,-0.00027)	(2.75,0.0)	0.20

Table III: Calculations for a Circular Jet

In the next stage of the analysis the effect of the finite thickness of the mixing region will be examined.

References

- BRIDGES, T. J. and MORRIS, P. J. (1984) Differential Eigenvalue Problems in Which the Parameter Appears Nonlinearly. *J. Comp. Phys.*, **55** (3) pp. 437-460.
- HANJALIC, K., LAUNDER, B. E. and SCHIESTEL, R. (1980) Multiple-Time-Scale Concepts in Turbulent Transport Modelling. *Turbulent Shear Flows II*, Springer-Verlag, pp. 36-49.
- KOMORI, S. and UEDA, H. (1985) The Large-Scale Coherent Structures in the Intermittent Region of the Self-Preserving Round Free Jet. *J. Fluid Mech.*, **152** pp. 337-359.
- MICHALKE, A. (1966) On Spatially Growing Disturbances in an Inviscid Shear Layer. *J. Fluid Mech.*, **23** pp. 521-544.

PATEL, R. P. (1973) An Experimental Study of a Plane Mixing Layer. *AIAA Journal*, **11** (1) pp. 67-71.

TAM, C. K. W., JACKSON, J. A. and SEINER, J. M. (1985) A Multiple Scales Model of the Shock Cell Structure of Imperfectly Expanded Supersonic Jets. *J. Fluid Mech.*, **153** pp. 123-149.